



ELSEVIER

Available online at www.sciencedirect.com

ScienceDirect

journal homepage: www.elsevier.com/locate/hydro

Facile synthesis and catalytic application of selenium doped graphene/CoFe₂O₄ for highly efficient and noble metal free dehydrogenation of formic acid

Yasamin Bide, Mohammad Reza Nabid*, Bahareh Etemadi

Department of Polymer, Faculty of Chemistry, Shahid Beheshti University, G.C., P.O. Box 1983969411, Tehran, Iran

ARTICLE INFO

Article history:

Received 10 May 2016

Received in revised form

1 August 2016

Accepted 17 August 2016

Available online xxx

Keywords:

Doped graphene

Selenium

CoFe₂O₄

Catalysis

Formic acid

ABSTRACT

The ongoing search for new noble metal free catalysts with excellent catalytic performance to replace homogeneous catalysts with difficult synthesis, separating and recycling and also expensive heterogeneous catalysts has been viewed as an important strategy to promote the development of hydrogen generation from formic acid. In this study, we reported the facile fabrication of selenium doped graphene/CoFe₂O₄ hybrid materials which exhibited excellent catalytic activity and magnetic recyclability for dehydrogenation of formic acid. Besides facilitating the catalyst isolation, CoFe₂O₄ nanoparticles have crucial role on the catalytic activity of the as-obtained material. Our results confirmed that combining CoFe₂O₄ with graphene is an effective strategy to inhibit metal oxide aggregation and synergistically improve the catalytic activity. Moreover, it is also demonstrated that selenium with large atomic size and high polarizability can enhance the catalytic activity of selenium doped graphene/CoFe₂O₄ hybrid materials.

© 2016 Hydrogen Energy Publications LLC. Published by Elsevier Ltd. All rights reserved.

Introduction

Formic acid (FA) has attracted considerable attention as a suitable liquid source for hydrogen (containing 4.4 wt.%, 53 g/L hydrogen) and hydrogen based green-energy applications because of the low toxicity, low cost, and high stability [1–5]. FA, which has been obtained in large quantities by the hydrogenation of waste carbon dioxide from industry, biomass processing, and artificial photosynthesis can undergo a catalytic dehydrogenation reaction, releasing H₂ that will be important for the generation of hydrogen in a more sustainable manner [6]. The main problem for practical applications

of this approach is the development of efficient catalysts. Recently, the dehydrogenation of FA is catalyzed by homogeneous organometallic catalysts with high selectivity and efficiency [7,8]. The difficulties in synthesis, controlling, separating and recycling are the main drawbacks of homogeneous catalysts preventing them for practical applications [3]. So, the development of heterogeneous catalysts with high performance for hydrogen generation from FA has recently been a hot topic [9]. Most of the reported heterogeneous catalysts include high cost and rare noble metals such as Au, Pd, and Pt which impede their practical applications [10,11]. So, the development of high-performance heterogeneous

* Corresponding author. Fax: +98 21 22431661.

E-mail address: m-nabid@sbu.ac.ir (M.R. Nabid).

<http://dx.doi.org/10.1016/j.ijhydene.2016.08.108>

0360-3199/© 2016 Hydrogen Energy Publications LLC. Published by Elsevier Ltd. All rights reserved.

catalysts without expensive noble metals for dehydrogenation of FA is urgently desired. Recently, bimetallic nanoparticles catalysts were shown to be more active than their single component counterparts for hydrogen generation from FA because of the charge redistribution between bimetals which reinforces the adsorption of formate through strong back donation [4].

From the point view of green chemistry, the practical approach to recover nanosized catalysts is a bottleneck for their applications. Compared with time-consuming procedures, such as filtration, centrifugation or gravitational separation, magnetic isolation leads to easier and better separation especially for small particles [12,13].

In the past two decades, magnetic cobalt ferrite (CoFe_2O_4), have attracted great attention in various fields such as electronics [14], catalysis [15–17], cancer therapy [18], and magnetic resonance imaging (MRI) [19] owing to its intrinsic nature of exhibiting magnetic hardness with high coercivity, high cubic magneto crystalline anisotropy, and moderate saturation magnetization [20]. However, due to the large surface area and strong dipole–dipole interactions, the pristine CoFe_2O_4 nanoparticles suffer from irreversibly aggregation. Among the various methods to reduce aggregation and settling, introduction of graphene oxide is expected to overcome these problems because of the large surface area, unique planar structure, low density, flexibility, chemical stability, and very high electrical conductivity [21]. On the other hand, by the combination of inorganic nanocrystals and graphene, such systems could have rich chemical/physical properties and also a possible synergistic effect [22–24]. Several groups have reported the synthesis of the cobalt ferrite/graphene nanocomposites employing different methods and also investigation of their application in various fields [25–27]. In 2015, Li et al. prepared light-weight sandwich-structured CoFe_2O_4 /graphene oxide hybrids by a facile one-pot polyol method followed by chemical conversion into FeCo/graphene hybrids for microwave absorber [28].

The introduction of foreign non-metallic atoms into graphene have been found to increase active sites, enhance the catalytic activity, and developing the electronic structure of graphene [29]. Recently, Se with similar electronegativity as carbon (selenium electronegativity: 2.55) was proposed as one of the attractive dopants for carbon materials because of its larger atomic size, inducing high strain at the edges of carbon materials and facilitating charge localization, as well as higher polarizability compared to S and facile interaction of lone Se pairs with the surrounding molecules [30,31]. In 2012, Yang et al. demonstrated that Se-graphene have better catalytic activity for the oxygen reduction reaction (ORR) than the commercial Pt/C in alkaline media which can potentially use for a substitute for Pt-based catalysts in fuel cells [32]. Jin et al. reported the fabrication and investigation of electrocatalytic performance of CNT/graphene doped with Se atoms, which shows excellent catalytic activity, long-term stability, and a high methanol tolerance [30].

It is important to note that, in continuation of our interest in different catalysts [33–37], though the present study provides a simple approach to achieve Se doped graphene CoFe_2O_4 hybrid materials as a noble metal free heterogeneous catalyst for hydrogen generation from FA. The influence of

CoFe_2O_4 , graphene and Se dopant on the catalytic activity have been investigated.

Experimental

Materials

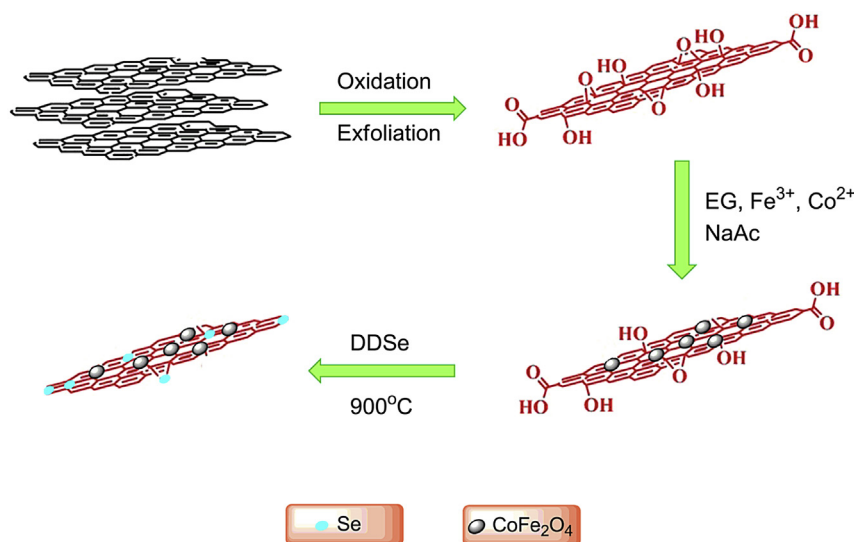
Graphite powder (325 mesh), sulfuric acid (H_2SO_4), potassium peroxydisulfate ($\text{K}_2\text{S}_2\text{O}_8$), di-phosphorus pentoxide (P_2O_5), potassium permanganate (KMnO_4), hydrogen peroxide (H_2O_2), ethylene glycol (EG), iron(III) chloride hexahydrate ($\text{FeCl}_3 \cdot 6\text{H}_2\text{O}$), cobalt(II) chloride hexahydrate ($\text{CoCl}_2 \cdot 6\text{H}_2\text{O}$), sodium acetate (NaAc), and diphenyl diselenide (DDSe) were purchased from Merck Chem. All other chemicals were purchased from Aldrich or Merck companies and used as received without any further purification.

Instruments and characterization

Fourier transform infrared (FT-IR) spectra were recorded on a Bomem MB-Series FT-IR spectrophotometer. Transmission electron microscopy (TEM) was performed by LEO 912AB electron microscope. Ultrasonic bath (EUROSONIC® 4D ultrasound cleaner with a frequency of 50 kHz and an output power of 350 W) was used to disperse materials in solvents. Thermogravimetric analysis (TGA) was carried out using STA 1500 instrument at a heating rate of $10\text{ }^\circ\text{C min}^{-1}$ in air. X-ray powder diffraction (XRD) data were collected on an XD-3A diffractometer using $\text{Cu K}\alpha$ radiation. X-ray photoelectron spectroscopy (XPS) was performed using a VG multilab 2000 spectrometer (ThermoVG scientific) in an ultrahigh vacuum. Ultraviolet–Visible (UV–Vis) spectra were obtained using a Shimadzu UV-2100 spectrophotometer. Scanning electron microscope (SEM) was performed on a Zeiss Supra 55 VP SEM instrument. AA-680 Shimadzu (Kyoto, Japan) flame atomic absorption spectrometer (AAS) with a deuterium background corrector was used for determination of the metal. The magnetization of the samples in a variable magnetic field was measured using a vibrating sample magnetometer (VSM) with a sensitivity of 10^{-3} EMU and a magnetic field of up to 8 kOe. The magnetic field was changed uniformly at a rate of 66 Oe s^{-1} . The gas chromatography (GC) analysis was performed on Shimadzu GC-2014 gas chromatograph.

Synthesis of graphene oxide (GO)

Graphene oxide (GO) was prepared through a modified Hummers method [38,39]. Graphite powders were first oxidized by sulfuric acid. Then 2.5 g of the graphite powder was treated with a solution by mixing 12.5 mL of concentrated H_2SO_4 with 2.5 g $\text{K}_2\text{S}_2\text{O}_8$ and 2.5 g P_2O_5 . The mixture was kept at $80\text{ }^\circ\text{C}$ for 6 h using a hotplate. Subsequently, the mixture was cooled to room temperature and diluted with 500 mL de-ionized (DI) water and left overnight. The mixture was then filtered and washed with DI water to remove the residual acid. The product was dried under ambient conditions overnight. The pretreated graphite powder was put into cold ($0\text{ }^\circ\text{C}$) concentrated H_2SO_4 (125 mL). Then KMnO_4 (15 g) was added gradually under stirring, and the temperature of the mixture was kept below



Scheme 1 – Schematic procedures to prepare selenium doped graphene/CoFe₂O₄.

20 °C by cooling. The mixture was then stirred at 35 °C for 4 h and then diluted with DI water (250 mL). Because adding water to concentrated sulfuric acid medium releases a large amount of heat, the dilution was carried out in an ice bath to keep the temperature below 50 °C. After adding all of the 250 mL DI water, the mixture was stirred for 2 h, and then an additional 750 mL DI water was added. Shortly thereafter, 20 mL 30% H₂O₂ was added to the mixture and the color of the mixture changed into brilliant yellow and began bubbling. The mixture was filtered and washed with 0.1 M HCl to remove metal ions, followed by 500 mL DI water to remove the acid. The resulting GO solid was dried in air.

Synthesis of graphene oxide/CoFe₂O₄ hybrid material

The graphene oxide/CoFe₂O₄ hybrid material was synthesized by a one-pot polyol method [28]. In a typical procedure, 40 mg GO was dispersed into 100 mL of ethylene glycol (EG) and ultrasounded for 3 h. 8 mmol FeCl₃·6H₂O and 4 mmol CoCl₂·6H₂O were added into the above suspension of GO and ultrasounded for another 3 h. 60 mmol NaAc was dissolved into the above solution. The solution was stirred and refluxed for 10 h. The black products were washed by water and ethanol for several times, and then dried in the atmospheric environment. For comparison purposes, pure CoFe₂O₄ nanocrystals were fabricated in the same approach without GO.

Synthesis of Se-doped graphene/CoFe₂O₄

Selenium doped graphene/CoFe₂O₄ was prepared by directly annealing GO/CoFe₂O₄ hybrid material and DDSe in argon [30]. In a typical procedure, GO/CoFe₂O₄ hybrid material (4 mg) was firstly ultrasonically dispersed in ethanol for about 90 min, and subsequently DDSe (4 mg) were added into the suspension under ultrasonic conditions. The resulting suspension was spread onto an evaporating dish and dried at 40 °C, forming a uniform solid mixture. The mixtures were placed into a quartz tube with an argon atmosphere and annealed at 900 °C for 3 h. After that, the sample was cooled to room

temperature under Ar ambient and collected from the quartz tube.

To investigate the effect of CoFe₂O₄ on the catalytic activity of the as-obtained material, selenium doped graphene was synthesized by a similar procedure and using GO instead of CoFe₂O₄ hybrid material.

Hydrogen generation from formic acid aqueous solution

An aqueous suspension containing the as-prepared catalyst was placed in a two-neck round-bottom flask, which was placed in a water bath under ambient atmosphere. A gas burette filled with water was connected to the reaction flask to measure the volume of released gas. The reaction was started when the mixed aqueous solution of FA was injected into the sealed flask to form a 4.5 mL of suspension. The molar ratio of CoFe/FA was fixed at 0.034 for all the catalytic reactions. The volume of the evolved gas was monitored by recording the displacement of water in the gas burette.

Results and discussion

Synthesis and recognition of the catalyst

The experimental scheme for preparation of selenium doped graphene/CoFe₂O₄ is illustrated in Scheme 1. In a typical procedure, the graphene oxide/CoFe₂O₄ hybrid material was synthesized by thermal decomposition of metal salts in the presence of GO with NaAc as a stabilizer and EG as the solvent through a facile one-pot polyol method. Owing to the abundant oxygen-containing functional groups on the surface of GO comprising carboxyl, hydroxyl and epoxy groups, GO is negatively charged. After adding Co and Fe salts to GO suspension, the electrostatic interaction between negative charge on GO and cobalt and iron cations lead to the in situ formation of CoFe₂O₄ magnetic nanoparticles on GO sheets. To prepare selenium doped graphene/CoFe₂O₄, GO and DDSe were first ultrasonically dispersed in ethanol. The resulting suspension

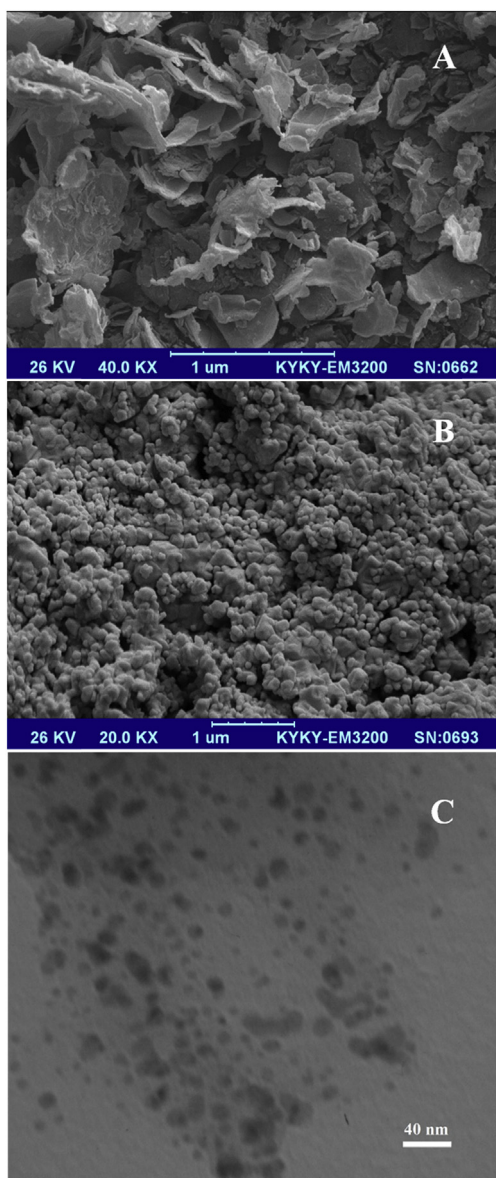


Fig. 1 – SEM images of GO (A) and Se-doped graphene/CoFe₂O₄, and TEM image of Se-doped graphene/CoFe₂O₄ (B and C).

was dried to form a uniform solid mixture and then placed in a quartz tube under an argon atmosphere and annealed at 900 °C. The amount of Co and Fe metals in the as-obtained catalyst were determined by AAS to be 1.5 and 3.7 mmol/g, respectively.

To investigate the morphology and structure of the materials, SEM and TEM images were provided. SEM image of GO clearly shows a crumpled flaky structure with a very low thickness (Fig. 1A). According to the SEM image of Se-doped graphene/CoFe₂O₄, after the introduction of CoFe₂O₄ nanoparticles, the GO sheets were homogeneously decorated by the nanoparticles (Fig. 1B). As shown in Fig. 1C, the thin and wrinkled GO nanosheets appears in TEM image of Se-doped graphene/CoFe₂O₄. Moreover, it can be observed that two-dimensional GO nanosheets are fully exfoliated and uniformly covered by a large number of spherical CoFe₂O₄

nanoparticles. From Fig. 1C the average particle size of CoFe₂O₄ was determined to be 14 nm. It is worth mentioning that almost no free CoFe₂O₄ nanoparticles are seen outside of GO nanosheets suggesting the strong interaction between CoFe₂O₄ and GO. So, SEM and TEM results confirm that CoFe₂O₄ nanoparticles are well wrapped by the graphene which lead to prevent the aggregation of CoFe₂O₄ NPs to a certain extent, which provides a great advantage for catalytic reactions.

XRD measurements were accomplished to investigate the phase and structure of the synthesized products (Fig. 2A). The XRD pattern of GO shows a diffraction peak at 2θ of 10.3°, related to (002) of GO, demonstrating the introduction of oxygen-based functional groups on the surface of the graphite. All the diffraction peaks of GO/CoFe₂O₄ can be assigned to a single phase of CoFe₂O₄ with a face-centered cubic spinel structure (JCPDS card No. 22-1086). The diffraction peaks at 2θ of 18.2°, 29.8°, 35.4°, 42.8°, 56.9° and 62.4° are related to (111), (220), (311), (400), (511) and (440) crystal planes of CoFe₂O₄, respectively. Moreover, because of destroying the regular layer stacking of GO by the crystal growth of CoFe₂O₄ between the interlayers and consequently the exfoliation of GO, the characteristic peak of GO is not observed in XRD pattern of GO/CoFe₂O₄. The average size of the CoFe₂O₄ nanoparticles were calculated to be 12.9 according to the Scherrer's formula which is consistent with TEM observations. In the XRD pattern of Se-doped graphene/CoFe₂O₄, all the diffraction peaks of CoFe₂O₄ are clearly observed which confirmed the retained morphology of nanoparticles after selenium doping.

FT-IR spectra of GO/CoFe₂O₄ and Se-doped graphene/CoFe₂O₄ samples are shown in Fig. 2B. For GO/CoFe₂O₄, the peaks at 3453, 1377 and 1070 cm⁻¹ are assigned to the –OH, C=O in carboxylic acid, and C–O stretching vibrations, respectively which confirm the existence of oxygen-containing functional groups on the surface of the nanosheets. Moreover, the peaks at 2921 and 2848 cm⁻¹ are ascribed to the asymmetric and symmetric stretching vibration of –CH₂, respectively. A prominent absorption band appeared at about 594 cm⁻¹ corresponds to the stretching mode of Fe(Co)–O [40]. The peak at 1631 cm⁻¹ is associated with the vibration of adsorbed water. In FT-IR spectrum of Se-doped graphene/CoFe₂O₄, most of the bands related with the oxygen-containing functional groups disappeared. It is revealed that the bulk of the oxygen-containing functional groups were removed from GO in the process of selenium doping thus the GO was effectively transformed into graphene in the synthesis. But the peak of Fe(Co)–O is still observed proving the successful synthesis of Se-doped graphene/CoFe₂O₄.

The magnetic properties of GO/CoFe₂O₄ and Se-doped graphene/CoFe₂O₄ were investigated by VSM at room temperature. The hysteresis loops are shown in Fig. 2C. The saturation magnetization (*M_s*) of GO/CoFe₂O₄ is about 45.4 emu/g [41]. The negligible remanence and coercivity in the magnetic hysteresis loops suggests the superparamagnetic behavior of GO/CoFe₂O₄. The magnetization curve of Se-doped graphene/CoFe₂O₄ indicate the ferromagnetic characteristics of as-prepared material and the coercivity is estimated to be ~500 Oe, proposing that the as obtained catalyst might be

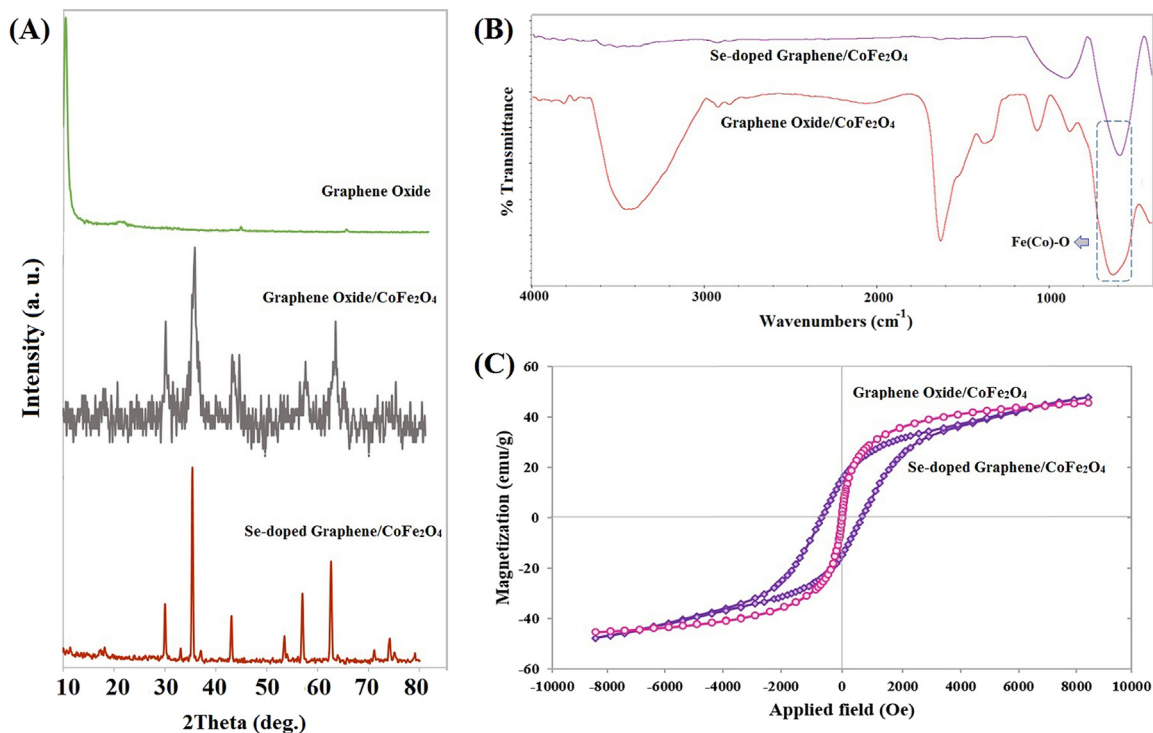


Fig. 2 – XRD patterns of GO, GO/CoFe₂O₄, and Se-doped graphene/CoFe₂O₄ (A), FT-IR spectra of GO/CoFe₂O₄ and Se-doped graphene/CoFe₂O₄ (B), and the field-dependent magnetization of GO/CoFe₂O₄ and Se-doped graphene/CoFe₂O₄ (C).

easily separated from solution phase through inducing an external magnetic field [42].

TGA and DTA curves of GO, GO/CoFe₂O₄ and Se-doped graphene/CoFe₂O₄ were obtained and presented in Fig. 3. In this experiment, the samples are heated to 780 °C under air atmosphere at a heating rate of 10 °C/min and a change in mass loss was recorded. TG analysis allows us to investigate thermal decomposition pattern and thermal stability of the as obtained materials. Three samples showed a slight weight loss below 120 °C, related to the evaporation of adsorbed water molecules. Thermogram of GO shows the weight losses between 120 and 205 °C due to the decomposition of labile oxygen-containing functional groups (such as C–O, C=O, etc.) [43], and another weight loss between 530 and 600 °C due to the thermal decomposition of the carbon skeleton [44]. After the introduction of CoFe₂O₄ nanoparticles to GO sheets, besides the weight loss due to the destruction of oxygenated functional groups of GO and removal of physically adsorbed water on CoFe₂O₄ nanoparticles at about 200 °C, a slight weight loss at 400 °C probably corresponds to the decomposition of surface adsorbed ethylene glycol is observed. In TGA curve of Se-doped graphene/CoFe₂O₄, almost no weight loss occurred because of the elimination of oxygen containing groups of GO after Se-doping.

Furthermore, the composition of Se-doped graphene/CoFe₂O₄ is also confirmed by XPS analysis (Fig. 4), which reveals the presence of C, O, Se, Fe, and Co on the surface of as-obtained material. The C 1s high resolution spectrum shows the peaks corresponding to sp² carbon atoms up-shifted to a higher binding energy (284.7 eV) than that of pristine graphene (284.5 eV) with Se introduction. The C1s XPS spectrum

can be divided into two different peaks, which correspond to the signals of C–C/C=C (284.7 eV), and C–O (285.5 eV). The O 1s XPS spectrum can be deconvoluted into two different peaks, chemical bindings which ascribed to the signals of C–OH or C–O–C (533.4 eV) and the lattice oxygen in the Co/Fe–O framework. 32–36 (531.5 eV) [45,46]. It can be observed that the high-resolution Se3d peak for Se-doped graphene/CoFe₂O₄ has an evidently binding energy at 56.5 eV due to C–Se–C bond in the Se-doped carbon similar to other literature for Se-doped carbon materials [30]. These results demonstrate that the bonds of Ph–Se–Se–Ph in DDSe were broken during the pyrolysis step, and the Se atoms were doped into the GO/CoFe₂O₄. According to the XPS results, selenium content in Se-doped graphene/CoFe₂O₄ is 1.59 at.%.

Catalytic activity

A sustainable and cost-effective approach for the release of H₂ from water solution of FA as a hydrogen source for practical applications (e.g. fuel cells) needs dehydrogenation reactions under the mild conditions without any additives and noble metals-based catalysts. So, we tested the activity of the Se-doped graphene/CoFe₂O₄ catalyst for the decomposition of FA in water (Fig. 5). The gas generation volume and rate over Se-doped graphene/CoFe₂O₄ catalyst are considerably influenced by the temperature and catalyst amount. To optimize the reaction conditions, we tested different temperatures and catalyst amounts as the results are summarized in Fig. 5. The dehydrogenation of FA at 60 °C with 0.007 g catalyst which released 110 mL of gas within 13 min was chosen as the optimized condition for further investigations.

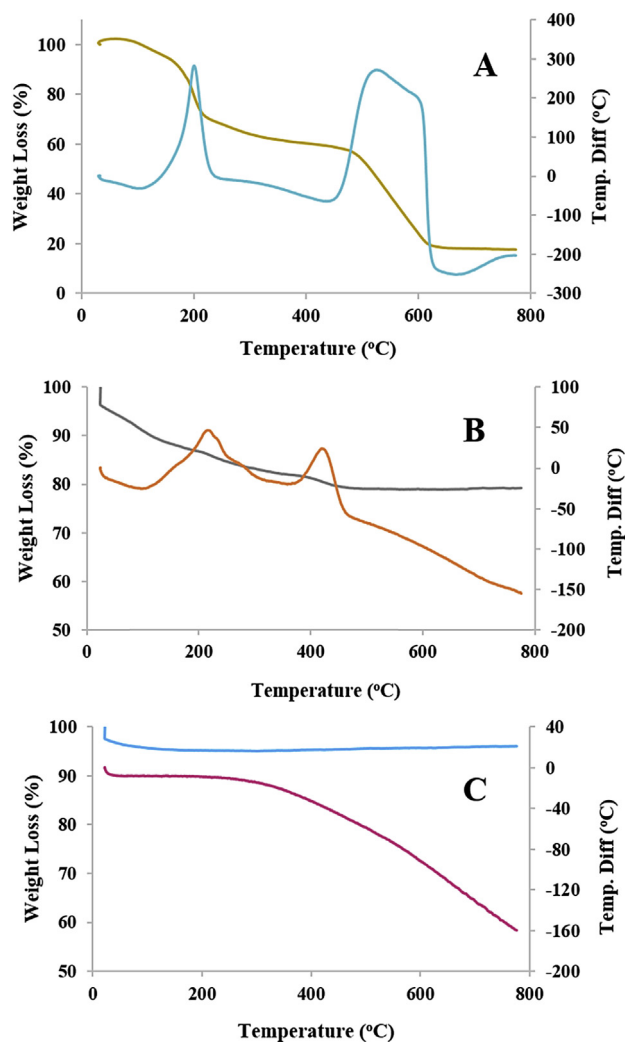


Fig. 3 – TGA and DTA curves of GO (A), GO/CoFe₂O₄ (B) and Se-doped graphene/CoFe₂O₄ (C).

It is noteworthy that the Se-doped graphene/CoFe₂O₄ gave a turnover frequency (TOF) of 306 h⁻¹, comparable to the most heterogeneous catalysts (Table S1), but without any additive and noble metals which make it unique among all previously reported catalysts.

To examine if graphene, Se dopants and CoFe₂O₄ have a dramatic effect on the catalytic performance, the as-synthesized GO, CoFe₂O₄, GO/CoFe₂O₄, Se-doped graphene together with the as-synthesized Se-doped graphene/CoFe₂O₄ were evaluated as catalysts for H₂ generation from FA decomposition. The results are given in Fig. 5. Se-doped graphene/CoFe₂O₄ clearly exhibits a much better activity than GO and GO/CoFe₂O₄ catalysts. That is, Se-doped graphene/CoFe₂O₄ exhibits much higher gas volume toward FA, which is more than two times compared to GO. From Fig. 6, it can be seen that the catalytic activity of GO/CoFe₂O₄ is much more than that of CoFe₂O₄, suggesting that the graphene plays a key role on the as-obtained hybrids. In a word, graphene was used as the support and the suspended bonds on the graphene oxide play an important role for the uniform distribution of CoFe₂O₄ nanoparticles during the synthesis. Besides, GO with

high migration efficiency of electrons has unique electronic structure which plays a vital role in improving the catalytic activity for hydrogen generation. Moreover, graphene can also prevent the aggregation and loss of activity of nanoparticles.

With Se introduction, the activity of Se-doped graphene/CoFe₂O₄ has been enhanced obviously compared to GO and GO/CoFe₂O₄. The enhanced catalytic activity with Se introduction can be attributed to several parameters. Firstly, the increased electron transfer due to restoring defects at carbon edges and formation of p conjugation system, secondly the induction of more strain in carbon materials owing to introduction of functional groups or doping atoms [47], as well as higher strain at the carbon edges due to the larger atomic size of Se than carbon, and thirdly higher polarizability of Se and interaction of lone selenium pairs with molecules in the surrounding media as compared with other heteroatoms such as N, P, or S. In addition, recent reports suggests that doping of graphite materials with large size atoms may be a promising approach to gain new metal free catalysts with high activity.

From Fig. 5, it is also obvious that CoFe₂O₄ nanoparticles are the crucial sites in the prepared catalyst. Namely, without CoFe₂O₄, Se-doped graphene shows much lower gas volume. The surface redox properties and Lewis acidity of CoFe₂O₄ due to the stabilizing effect of Co on the distribution of iron sites probably cause the enhanced ability of FA adsorption and O–H bond polarization on the binary spinel [48,49], which leads to its catalytic behavior in FA decomposition.

Another pathway for the decomposition of FA is a dehydration reaction which lead to release of CO. To investigate the possibility of this undesired reaction, a trap containing limewater was used to remove CO₂ from the as formed gas of the catalytic reaction. A loss of around 50% in volume was observed suggesting a volume ratio of CO₂ and H₂ to be 1:1 in the as-formed gas. Moreover, analysis by GC further confirmed that the gas treated with the limewater was pure hydrogen with no CO (Fig. S1).

Being highly stable, easily separable, and readily recyclable are very important for practical application of catalysts. We tested the durability of the Se-doped graphene/CoFe₂O₄ catalyst in the decomposition of FA at 60 °C (Fig. S2). The results showed a slight decrease in the productivity of hydrogen after six runs mainly ascribed to the slightly increased particle size of the CoFe₂O₄ NPs. Moreover, XRD measurement of the recovered catalyst show no significant change in the structure of the catalyst, exhibiting high durability and stability of the catalyst (Fig. S3). Moreover, the catalyst could easily be isolated from the reaction mixture by simply using magnet removing the need for filtration/centrifugation which the complete catalyst recovery is usually not possible. According to the results, the presented catalyst has a great potential for practical large scale and sustainable applications.

Conclusion

In summary, we have developed a noble metal free magnetic catalyst for dehydrogenation of formic acid that exhibits high efficiency in aqueous solution under the mild conditions. CoFe₂O₄ NPs were synthesized onto graphene oxide sheets and then selenium doping was accomplished to obtain the Se-

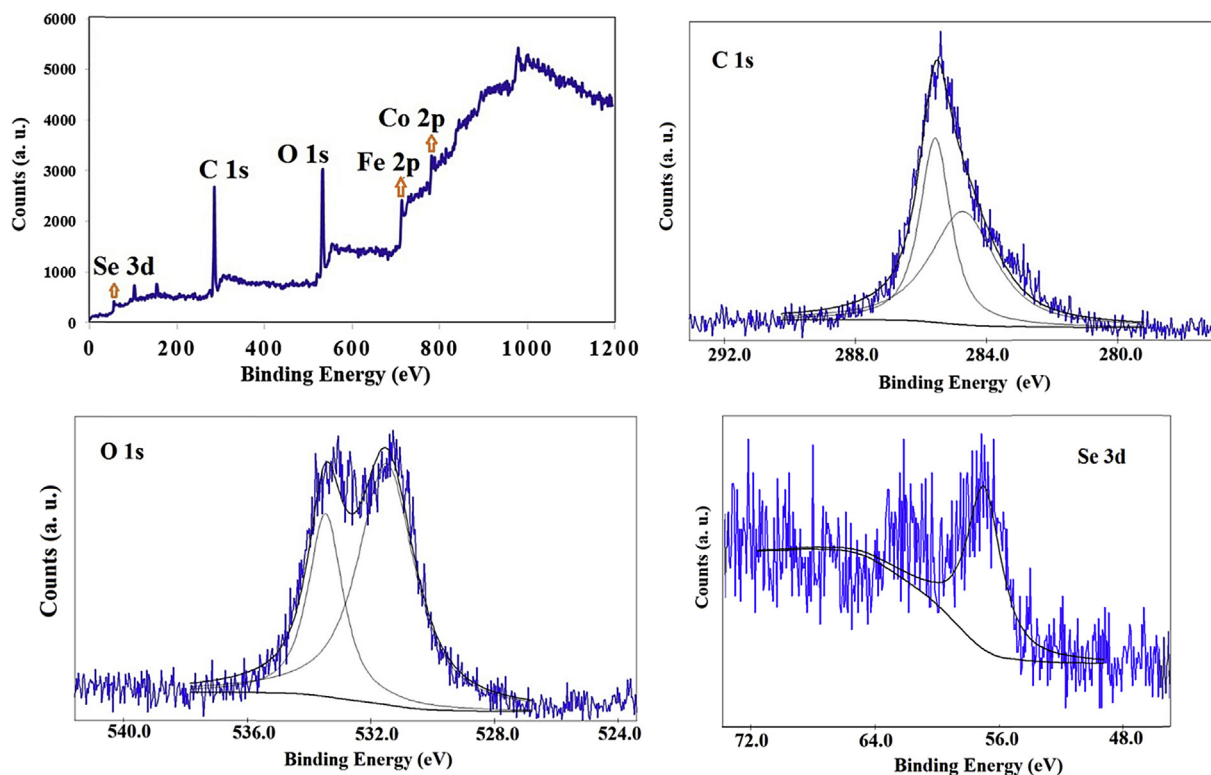


Fig. 4 – XPS spectrum of Se-doped graphene/CoFe₂O₄, and high resolution XPS spectra of C 1s, O 1s and Se 3d.

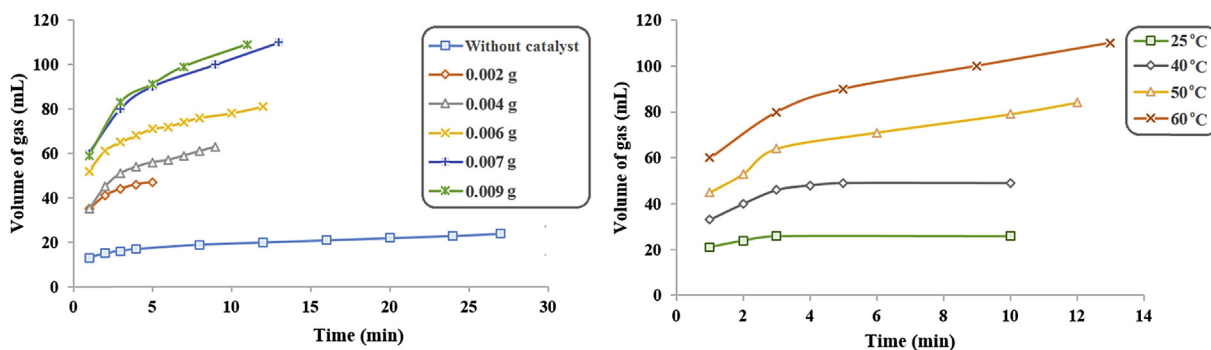


Fig. 5 – The effect of temperature and catalyst amount on gas generation (60 °C for optimization of catalyst amount, and 0.007 g catalyst for optimization of temperature).

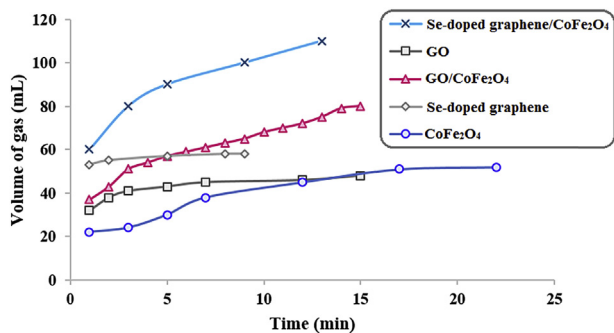


Fig. 6 – Volume of the generated gas versus time for the dehydrogenation of FA over GO, CoFe₂O₄, GO/CoFe₂O₄, Se-doped graphene and Se-doped graphene/CoFe₂O₄ (0.007 g catalyst, 60 °C).

doped graphene/CoFe₂O₄. Various characterization techniques such as SEM, TEM, FT-IR, XRD, TGA, XPS and VSM were performed to confirm the formation of as-obtained materials. According to the results, Se-doped graphene/CoFe₂O₄ exhibited better catalytic activity than pure CoFe₂O₄, GO, Se-doped graphene and GO/CoFe₂O₄ hybrid materials which the possible explanations were presented. The suggested catalyst provides a cost-effective, environmentally friendly and noble metal free catalyst with relatively good activity compared to most of reported heterogeneous catalysts for dehydrogenation of formic acid. In addition, the catalyst showed very good durability, stability and also fast and complete recovery by magnetic extraction representing new potentials for the development of more sustainable catalysts for green energy systems.

Acknowledgments

The financial support provided by the Iran National Science Foundation (INSF) is gratefully acknowledged.

Appendix A. Supplementary data

Supplementary data related to this article can be found at <http://dx.doi.org/10.1016/j.ijhydene.2016.08.108>.

REFERENCES

- [1] An L, Yan H, Li B, Ma J, Wei H, Xia D. Highly active N–PtTe/reduced graphene oxide intermetallic catalyst for formic acid oxidation. *Nano Energy* 2015;15:24–32.
- [2] Wang Z-L, Yan J-M, Wang H-L, Ping Y, Jiang Q. Pd/C synthesized with citric acid: an efficient catalyst for hydrogen generation from formic acid/sodium formate. *Sci Rep* 2012;2:598.
- [3] Metin Ö, Sun X, Sun S. Monodisperse gold–palladium alloy nanoparticles and their composition-controlled catalysis in formic acid dehydrogenation under mild conditions. *Nanoscale* 2013;5:910–2.
- [4] Guo WL, Li L, Li LL, Tian S, Liu SL, Wu YP. Hydrogen production via electrolysis of aqueous formic acid solutions. *Int J Hydrogen Energy* 2011;36:9415–9.
- [5] Singh AK, Singh S, Kumar A. Hydrogen energy future with formic acid: a renewable chemical hydrogen storage system. *Catal Sci Technol* 2016;6:12–40.
- [6] Johnson TC, Morris DJ, Wills M. Hydrogen generation from formic acid and alcohols using homogeneous catalysts. *Chem Soc Rev* 2010;39:81–8.
- [7] Sponholz P, Mellmann D, Junge H, Beller M. Towards a practical setup for hydrogen production from formic acid. *ChemSusChem* 2013;6:1172–6.
- [8] Thevenon A, Frost-Pennington E, Weijia G, Dalebrook AF, Laurenczy G. Formic acid dehydrogenation catalysed by tris (TPPTS) ruthenium species: mechanism of the initial “fast” cycle. *ChemCatChem* 2014;6:3146–52.
- [9] Zhou X, Huang Y, Liu C, Liao J, Lu T, Xing W. Available hydrogen from formic acid decomposed by rare earth elements promoted Pd–Au/C catalysts at low temperature. *ChemSusChem* 2010;3:1379–82.
- [10] Bulushev DA, Jia L, Beloshapkin S, Ross JR. Improved hydrogen production from formic acid on a Pd/C catalyst doped by potassium. *Chem Commun* 2012;48:4184–6.
- [11] Liu J, Lan L, Li R, Liu X, Wu C. Agglomerated Ag–Pd catalyst with performance for hydrogen generation from formic acid at room temperature. *Int J Hydrogen Energy* 2016;41:951–8.
- [12] Rocher V, Bee A, Siaugue J-M, Cabuil V. Dye removal from aqueous solution by magnetic alginate beads crosslinked with epichlorohydrin. *J Hazard Mater* 2010;178:434–9.
- [13] Tang M, Xia F, Gao C, Qiu H. Preparation of magnetically recyclable CuFe₂O₄/RGO for catalytic hydrolysis of sodium borohydride. *Int J Hydrogen Energy* 2016;41:13058–68.
- [14] Nappini S, Magnano E, Bondino F, Pís I, Barla A, Fantechi E, et al. Surface charge and coating of CoFe₂O₄ nanoparticles: evidence of preserved magnetic and electronic properties. *J Phys Chem C* 2015;119:25529–41.
- [15] Zhang Z, Jiang Y, Chi M, Yang Z, Nie G, Lu X, et al. Fabrication of Au nanoparticles supported on CoFe₂O₄ nanotubes by polyaniline assisted self-assembly strategy and their magnetically recoverable catalytic properties. *Appl Surf Sci* 2016;363:578–85.
- [16] Zhang M, Lu J, Zhang J-N, Zhang Z-H. Magnetic carbon nanotube supported Cu (CoFe₂O₄/CNT–Cu) catalyst: a sustainable catalyst for the synthesis of 3-nitro-2-arylimidazo [1, 2-a] pyridines. *Catal Commun* 2016;78:26–32.
- [17] Li PH, Li BL, An ZM, Mo LP, Cui ZS, Zhang ZH. Magnetic nanoparticles (CoFe₂O₄)-supported phosphomolybdate as an efficient, green, recyclable catalyst for synthesis of β -hydroxy hydroperoxides. *Adv Synth Catal* 2013;355:2952–9.
- [18] Matsuda S, Nakanishi T, Kaneko K, Osaka T. Synthesis of cobalt ferrite nanoparticles using spermine and their effect on death in human breast cancer cells under an alternating magnetic field. *Electrochim Acta* 2015;183:153–9.
- [19] Nidhin M, Nazeer SS, Jayasree RS, Kiran MS, Nair BU, Sreeram KJ. Flower shaped assembly of cobalt ferrite nanoparticles: application as T2 contrast agent in MRI. *RSC Adv* 2013;3:6906–12.
- [20] Ammar S, Helfen A, Jouini N, Fievet F, Rosenman I, Villain F, et al. Magnetic properties of ultrafine cobalt ferrite particles synthesized by hydrolysis in a polyol medium. *J Mater Chem* 2001;11:186–92.
- [21] Kamat PV. Graphene-based nanoarchitectures. Anchoring semiconductor and metal nanoparticles on a two-dimensional carbon support. *J Phys Chem Lett* 2009;1:520–7.
- [22] Huang X, Qi X, Boey F, Zhang H. Graphene-based composites. *Chem Soc Rev* 2012;41:666–86.
- [23] Ma X, Tao H, Yang K, Feng L, Cheng L, Shi X, et al. A functionalized graphene oxide-iron oxide nanocomposite for magnetically targeted drug delivery, photothermal therapy, and magnetic resonance imaging. *Nano Res* 2012;5:199–212.
- [24] Li X, Zhu H, Feng J, Zhang J, Deng X, Zhou B, et al. One-pot polyol synthesis of graphene decorated with size- and density-tunable Fe₃O₄ nanoparticles for porcine pancreatic lipase immobilization. *Carbon* 2013;60:488–97.
- [25] Fu Y, Chen H, Sun X, Wang X. Combination of cobalt ferrite and graphene: high-performance and recyclable visible-light photocatalysis. *Appl Catal B* 2012;111:280–7.
- [26] Xia H, Zhu D, Fu Y, Wang X. CoFe₂O₄-graphene nanocomposite as a high-capacity anode material for lithium-ion batteries. *Electrochim Acta* 2012;83:166–74.
- [27] Wang G, Ma Y, Dong X, Tong Y, Zhang L, Mu J, et al. Facile synthesis and magnetorheological properties of superparamagnetic CoFe₂O₄/GO nanocomposites. *Appl Surf Sci* 2015;357:2131–5.
- [28] Li X, Feng J, Zhu H, Qu C, Bai J, Zheng X. Sandwich-like graphene nanosheets decorated with superparamagnetic CoFe₂O₄ nanocrystals and their application as an enhanced electromagnetic wave absorber. *RSC Adv* 2014;4:33619–25.
- [29] Kong X-K, Chen C-L, Chen Q-W. Doped graphene for metal-free catalysis. *Chem Soc Rev* 2014;43:2841–57.
- [30] Jin Z, Nie H, Yang Z, Zhang J, Liu Z, Xu X, et al. Metal-free selenium doped carbon nanotube/graphene networks as a synergistically improved cathode catalyst for oxygen reduction reaction. *Nanoscale* 2012;4:6455–60.
- [31] Choi CH, Chung MW, Jun YJ, Woo SI. Doping of chalcogens (sulfur and/or selenium) in nitrogen-doped graphene–CNT self-assembly for enhanced oxygen reduction activity in acid media. *RSC Adv* 2013;3:12417–22.
- [32] Yang Z, Yao Z, Li G, Fang G, Nie H, Liu Z, et al. Sulfur-doped graphene as an efficient metal-free cathode catalyst for oxygen reduction. *ACS Nano* 2011;6:205–11.
- [33] Bide Y, Nabid MR, Dastar F. Poly(2-aminothiazole) as a unique precursor for nitrogen and sulfur co-doped porous carbon: immobilization of very small gold nanoparticles and its catalytic application. *RSC Adv* 2015;5:63421–8.
- [34] Nabid MR, Bide Y, Dastar F. One pot synthesis of nickel nanoparticles stabilized on rGO/polyethyleneimine aerogel

- for the catalytic hydrogen generation. *Catal Lett* 2015;145:1798–807.
- [35] Nabid MR, Bide Y, Habibi Z. Synthesis of a yolk/shell Fe_3O_4 @poly (ionic liquid) s-derived nitrogen doped graphitic porous carbon materials and its application as support for nickel catalysts. *RSC Adv* 2015;5:2258–65.
- [36] Nabid MR, Bide Y. H40-PCL-PEG unimolecular micelles both as anchoring sites for palladium nanoparticles and micellar catalyst for Heck reaction in water. *Appl Catal A* 2014;469:183–90.
- [37] Nabid MR, Bide Y, Niknezhad M. Fe_3O_4 – SiO_2 –P4VP pH-sensitive microgel for immobilization of nickel nanoparticles: an efficient heterogeneous catalyst for nitrile reduction in water. *ChemCatChem* 2014;6:538–46.
- [38] Hummers Jr WS, Offeman RE. Preparation of graphitic oxide. *J Am Chem Soc* 1958;80:1339.
- [39] Jung JH, Cheon DS, Liu F, Lee KB, Seo TS. A graphene oxide based immuno-biosensor for pathogen detection. *Angew Chem Int Ed* 2010;49:5708–11.
- [40] He G, Ding J, Zhang J, Hao Q, Chen H. One-step ball-milling preparation of highly photocatalytic active CoFe_2O_4 –reduced graphene oxide heterojunctions for organic dye removal. *Ind Eng Chem Res* 2015;54:2862–7.
- [41] Li X, Feng J, Du Y, Bai J, Fan H, Zhang H, et al. One-pot synthesis of CoFe_2O_4 /graphene oxide hybrids and their conversion into FeCo/graphene hybrids for lightweight and highly efficient microwave absorber. *J Mater Chem A* 2015;3:5535–46.
- [42] Li N, Zheng M, Chang X, Ji G, Lu H, Xue L, et al. Preparation of magnetic CoFe_2O_4 -functionalized graphene sheets via a facile hydrothermal method and their adsorption properties. *J Solid State Chem* 2011;184:953–8.
- [43] Sui Z-Y, Cui Y, Zhu J-H, Han B-H. Preparation of three-dimensional graphene oxide–polyethylenimine porous materials as dye and gas adsorbents. *ACS Appl Mater Interfaces* 2013;5:9172–9.
- [44] Du F-P, Wang J-J, Tang C-Y, Tsui C-P, Zhou X-P, Xie X-L, et al. Water-soluble graphene grafted by poly (sodium 4-styrenesulfonate) for enhancement of electric capacitance. *Nanotechnology* 2012;23:475704.
- [45] Liu S, Bian W, Yang Z, Tian J, Jin C, Shen M, et al. A facile synthesis of CoFe_2O_4 /biocarbon nanocomposites as efficient bi-functional electrocatalysts for the oxygen reduction and oxygen evolution reaction. *J Mater Chem A* 2014;2:18012–7.
- [46] Lee DU, Kim BJ, Chen Z. One-pot synthesis of a mesoporous NiFe_2O_4 nanoplatelet and graphene hybrid and its oxygen reduction and evolution activities as an efficient bi-functional electrocatalyst. *J Mater Chem A* 2013;1:4754–62.
- [47] Ji L, Rao M, Zheng H, Zhang L, Li Y, Duan W, et al. Graphene oxide as a sulfur immobilizer in high performance lithium/sulfur cells. *J Am Chem Soc* 2011;133:18522–5.
- [48] Manova E, Tsoncheva T, Paneva D, Mitov I, Tenchev K, Petrov L. Mechanochemically synthesized nano-dimensional iron–cobalt spinel oxides as catalysts for methanol decomposition. *Appl Catal A* 2004;277:119–27.
- [49] Lázár K, Mathew T, Koppány Z, Megyeri J, Samuel V, Mirajkar SP, et al. $\text{Cu}_{1-x}\text{Co}_x\text{Fe}_2\text{O}_4$ ferros spinels in alkylation: structural changes upon reaction. *Phys Chem Chem Phys* 2002;4:3530–6.